Article

Evaluation of Cyclic Healing Potential of Bacteria-Based Self-Healing Cementitious Composites

Ismael Justo-Reinoso [1],[*] , Bianca J. Reeksting [2], Andrew Heath [1], Susanne Gebhard [2] and Kevin Paine [1]

1   Centre for Innovative Construction Materials, Department of Architecture and Civil Engineering,
     University of Bath, Bath BA2 7AY, UK; a.heath@bath.ac.uk (A.H.); k.paine@bath.ac.uk (K.P.)
2   Milner Centre for Evolution, Department of Biology and Biochemistry, University of Bath, Bath BA2 7AY, UK;
     b.j.reeksting@bath.ac.uk (B.J.R.); s.gebhard@bath.ac.uk (S.G.)
*   Correspondence: ijr27@bath.ac.uk

Abstract: At present, little evidence exists regarding the capability of bacteria-based self-healing (BBSH) cementitious materials to successfully re-heal previously healed cracks. This paper investigates the repeatability of the self-healing of BBSH mortars when the initially healed crack is reopened at a later age (20 months) and the potential of encapsulated bacterial spores to heal a new crack generated at 22 months after casting. The results show that BBSH cement mortar cracks that were successfully healed at an early age were not able to successfully re-heal when cracks were reformed in the same location 20 months later, even when exposed to favourable conditions (i.e., high humidity, temperature, calcium source, and nutrients) to promote their re-healing. Therefore, it is likely that not enough bacterial spores were available within the initially healed crack to successfully start a new self-healing cycle. However, when entirely new cracks were intentionally generated at a different position in 22-month-old mortars, these new cracks were able to achieve an average healing ratio and water tightness of 93.3% and 90.8%, respectively, thus demonstrating that the encapsulated bacterial spores remained viable inside the cementitious matrix. The results reported in this paper provide important insights into the appropriate design of practical self-healing concrete and, for the first time, show limitations of the ability of BBSH concrete to re-heal.

Keywords: bacteria; biomineralization; cyclic healing; later age; MICP; re-healing; self-healing concrete

1. Introduction

In recent decades, the construction industry has heavily depended on concrete because of its mechanical properties, cost-effective production, and ease of application. Nevertheless, cracks tend to form in concrete due to its limited tensile strength [1,2]. Concrete is usually combined with steel reinforcement to bear the tensile stresses and limit crack width. However, even the use of this reinforcement steel cannot completely prevent the formation of cracks. Cracks in concrete allow the deep penetration of detrimental agents and water in the structure, accelerating the corrosion of the reinforcement steel and inducing a rapid deterioration of concrete structures. To counteract the adverse effects of cracks on the service life of concrete structures, there has been a significant effort over the past decade to develop innovative self-healing cementitious materials able to repair cracks by themselves. Among the different self-healing technologies investigated to fulfil this aim, the use of bacteria to induce the precipitation of calcium carbonates has attracted interest not only due to the efficient bonding capacity and compatibility with the cement matrix that it achieves [3,4] but also for its environmental advantages [5]. This technology relies on microbially induced calcite precipitation (MICP) [4,6,7]. However, not all bacteria can survive in the harsh alkaline conditions present in the cement matrix. In this context, alkaliphilic bacteria able to thrive and precipitate calcium carbonates in high pH environments have been isolated from different locations around the world to develop bacteria-based self-healing (BBSH)

cementitious composites [8–10]. *Bacillus* and *Sporosarcina* species have been the preferred options not only for their ability to grow in high pH environments and create efficient conditions for calcium carbonate precipitation [11] but also for their capability to form spores, which are durable forms of bacteria that can survive harsh conditions for many years [12,13]. Bacterial spores are used instead of vegetative cells as they can remain in a dormant phase for years before the presence of water and oxygen in a newly formed crack stimulates their germination. However, spores need to be protected from the initial mixing conditions and during the hardening phase of cementitious materials. For this purpose, different protection methods have been proposed to guarantee that enough viable spores will activate when new cracks are formed. These protection methods include microencapsulation [4,14,15], porous particles [16–18], superabsorbent polymers [19,20], surfactants [21–23], and powder-compressed particles [24], among others.

However, to date, most research conducted on BBSH cementitious composites has been focused on the initial healing capacity of these systems when a crack is formed at an early age (typically 28 days) [5,9,16]. Therefore, the long-term survival rate of encapsulated bacterial spores still remains unclear [25]. This leaves a knowledge gap regarding the performance of these BBSH systems when cracks are formed for the first time after a more extended period (i.e., more than one year). Moreover, cyclic loading can cause previously healed cracks to be reopened, once again allowing harmful agents to directly access the steel reinforcement. In this context, the repeatability of the healing ability has not yet been properly addressed [4], and only a few studies have investigated the effectiveness of BBSH systems under repeated cracking and healing cycles (self-healing repeatability) [26]. No previous research has addressed the self-healing repeatability when these cracks, initially self-healed at an early age (i.e., 28 days), are reopened more than one year later. Therefore, it is crucial to fill this knowledge gap to better understand the behaviour of these BBSH cementitious composites when previously successfully healed cracks are reformed after more than a year.

The present work has two principal objectives: on the one hand, to investigate the repeatability of the self-healing of BBSH mortars when the initially healed crack is reformed at a later age (20 months); and on the other hand, to assess the potential of encapsulated bacterial spores to heal a new crack generated at 22 months.

2. Materials and Methods

2.1. Preparation of Mortar Prisms

The complete information regarding the materials and methods followed for the endospore production, preparation of mortar prisms, and healing performance results of the mortar prisms used in this study can be found in the work of Reeksting et al. [9]. For the sake of completeness, the main information is also included in this section.

2.1.1. Bacterial Isolates

Spores from the bacterium MM1_1 DSM 110489 (closely related to *Bacillus licheniformis*) were used by Reeksting et al. [9] to produce the bacteria-based mortar prisms investigated in this study. These spore-forming bacteria were collected from a limestone bedrock in the southwest of the United Kingdom. The procedures for culturing, growing, and forming spores for the present study were carried out as described in this previous work [9].

2.1.2. Growth Medium (GM)

The growth medium (GM) used to produce the mortar prisms contained calcium nitrate and yeast extract at 5% and 1% of the cement mass, respectively [9]. Calcium nitrate and yeast extract were obtained from Sigma-Aldrich Corporation (UK). The GM was added directly to the mixing water.

2.1.3. Aerated Concrete Granules (ACGs)

The aerated concrete granules (ACGs) were supplied by Cellumat SA (Belgium) and sieved to obtain the desired particle size distribution of 1–4 mm. The ACGs had an absorption capacity and loose dry bulk density of 120% and 354 kg/m^3, respectively [16]. MM1_1 spores (2.1×10^{10} CFU) were added to a volume of water equal to the total water absorption capacity of 3.54 g of ACG particles. Then, ACG particles were saturated entirely with this bacterial spore suspension using a vacuum saturation technique, as fully described in [16]. ACG particles were then dried and sealed with polyvinyl acetate (PVA) (30% wt./wt.) [9]. ACG particles sealed with PVA but without spores (ACG-NS) were produced for Control samples. The PVA-coated ACG particles containing spores (ACG-S) and without spores (ACG-NS) were placed in Ziploc®-type plastic bags until used in mortar mixes.

2.1.4. Casting of Mortar Prisms

Mortar prisms (65 mm $\times$ 40 mm $\times$ 40 mm) of the three mixes investigated in this study (i.e., Reference, Control, and Bio) were initially prepared by Reeksting et al. [9]. The Reference mix was a plain mortar mix where no ACG particles (with or without bacterial spores) nor GM were added. The Bio mix contained GM and bacterial spores encapsulated into ACG particles (ACG-S), while the Control mix contained GM and ACG particles without bacterial spores (ACG-NS). All the mortar mixes were prepared in triplets and cast in two layers (20 mm each). The mix proportions for the first layer (bottom layer) are shown in Table 1. A Portland-limestone cement (i.e., CEM II/A-L 32.5R) and standard sand were used conforming to BS EN 197-1 and BS EN 196-1, respectively. Tap water was used to achieve a water/cement ratio of 0.5. Mixing was carried out following BS EN 196-1. PVA-coated ACG particles containing bacterial spores were dry mixed with the sand and then added simultaneously with the sand, while the GM (i.e., calcium nitrate and yeast extract) was added directly with the mixing water. In the Control and Bio mixes, a part of the sand content was replaced (by volume) to consider the inclusion of ACG particles (ACG-S or ACG-NS), calcium nitrate, and yeast extract. After approximately 3 h, the second layer (top layer) containing standard cement mortar was cast following the mix proportions given for the Reference mix in Table 1.

Table 1. Mix proportions for the mortar samples.

Mix	Cement (g)	Water (mL)	Sand (g)	Calcium Nitrate (g)	Yeast Extract (g)	Bacterial Spores (CFU)	PVA-Coated ACG-S (g)	PVA-Coated ACG-NS (g)
Reference	92	46	276	0	0	0	0	0
Control	92	46	253	4.6	1.0	0	0	4.6
Bio	92	46	253	4.6	1.0	2.1×10^{10}	4.6	0

Mortar prisms were demoulded after 24–48 h and immediately cured for 28 days submerged in tap water at room temperature (i.e., 20 $\pm$ 5 °C). After curing for 28 days, the mortar prisms were oven-dried for 24 h at 50 °C. Then, the top half (standard cement mortar layer) was wrapped with carbon fibre-reinforced polymer strips. A notch of approximately 1.5 mm depth was sawn at the centre of each mortar prism (bottom layer) to induce crack formation. Mortar prisms were cracked under three-point bending using a 30-kN Instron static testing frame. The load was applied to maintain a crack growth of 0.025 mm per minute. Crack width was measured using a crack mouth opening displacement (CMOD) gauge, and loading was stopped when the crack width was predicted to be 0.5 mm after releasing the load. After cracking, the mortar prisms of each mortar mix were placed in separate plastic containers to avoid cross-contamination. The plastic containers were filled with tap water to 10 mm below the top of the mortars with the crack and then incubated at

room temperature for two months. Containers were open to the atmosphere during the incubation process.

The healing ratios initially obtained by Reeksting et al. [9] for the mortar prisms are shown in Table 2. Healing ratios (%) were obtained as a function of the recovery of water tightness. These same mortar specimens were used in this study to evaluate the self-healing ability (i) after re-cracking of previously healed cracks at a later age (i.e., 20 months) and (ii) with the formation of new cracks in 22-month-old mortar prisms.

Table 2. Healing ratio percentages observed by Reeksting et al. [9] when the mortar prisms used in this study were cracked initially at 28 days and healed for 8 weeks. Healing ratio (%) was obtained as a function of the recovery of water tightness.

Mortar Mix	Sample	Healing Ratio (%)
Reference	Ref 1	21.4
	Ref 2	35.7
	Ref 3	35.3
Control	Ctrl 1	70.0
	Ctrl 2	99.5
	Ctrl 3	99.9
Bio	Bio 1	99.8
	Bio 2	99.7
	Bio 3	92.2

In Figure 1, a schematic flowchart diagram presents the different steps involving the mortar prisms investigated in this study, from the casting, curing, cracking, and healing process initially conducted by Reeksting et al. [9] to the re-cracking and formation of new cracks at 20 and 22 months, respectively.
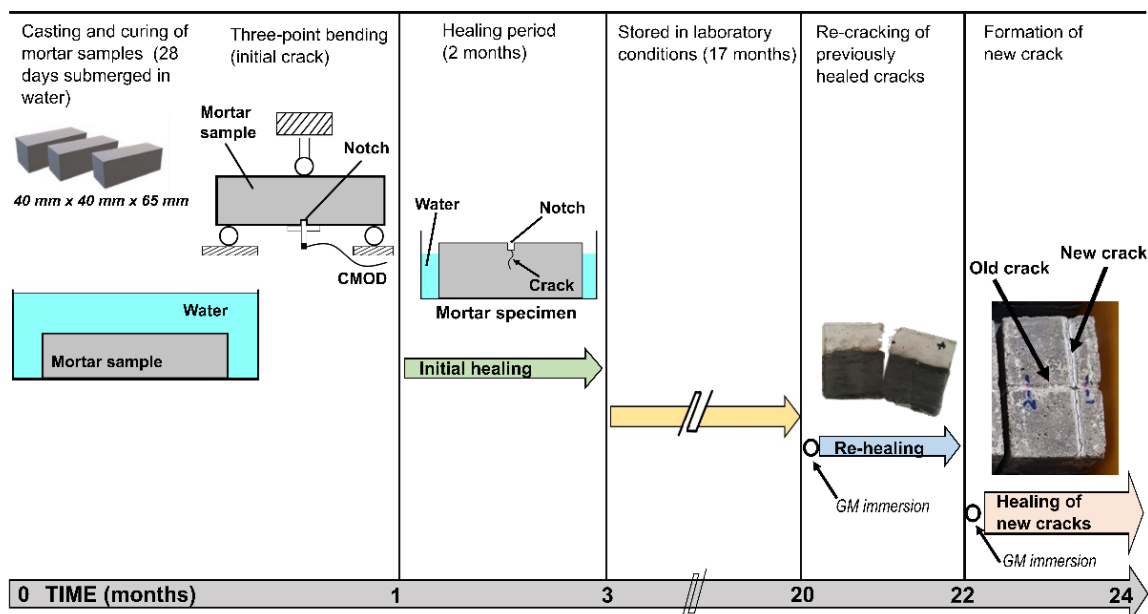

Figure 1. Schematic flowchart showing the different steps followed to investigate the repeatability of the self-healing of BBSH mortars when the initially healed crack is reformed at a later age (20 months) and the potential of encapsulated bacterial spores to heal a new crack formed at 22 months after casting. GM = growth medium.

2.2. Re-Cracking of Previously Healed 20-Month-Old Mortar Prisms

To evaluate the capacity of bacteria to re-heal previously healed cracks (~0.5 mm width), the healed mortar prisms were re-cracked at the age of 20 months. Three-point bending was used to reopen the healed crack to a width of approximately 0.5 mm on the removal of the load. A 30-kN Instron static testing frame was used to apply the load necessary to maintain a crack growth of 0.025 mm per minute. Crack width was measured using a CMOD gauge, and loading was stopped when the crack width was 0.7 mm. Before releasing the load, plastic spacers with 0.5 mm thickness were placed at both ends of the reopened crack to control the crack width.

As the mortar prisms were initially exposed to alternate wetting and drying periods during their healing process and then exposed for 17 months to laboratory conditions (i.e., 20 °C, RH ~50%), the mortar prisms were continuously exposed to environmental CO_2, likely resulting in carbonation [1,27]. Tan et al. [16] demonstrated that the self-healing of cementitious materials that crack after carbonation is almost totally dependent on the supply of calcium ions from an encapsulated source that are released when the crack is formed, as calcium hydroxide from the cement matrix itself is not readily available after carbonation. Therefore, to ensure that the spores within the previously healed crack would have access to the nutrients and calcium sources needed to induce the precipitation of new $CaCO_3$ precipitates in the reopened crack, the half containing the crack was submerged after re-cracking in a growth medium (GM) solution for 5 h. This GM solution contained yeast extract (4 g/L) and calcium nitrate (50 g/L) with a pH adjusted to 11 using a 1 M NaOH solution. The mortar prisms of each mortar mix were submerged in the GM using separate plastic containers to avoid cross-contamination. After the nutrients/calcium solution immersion period, the samples were left to dry overnight at room temperature (20 °C) with the crack facing upwards. Following overnight drying, mortar prisms were placed in containers open to the atmosphere and filled with tap water to 10 mm below the top of the mortars, and then incubated at room temperature for 5 weeks. Samples were placed in separate containers to avoid any cross-contamination between samples. Originally marked with a permanent black marker pen, two specific crack locations were monitored during this study for each specimen. Photos of the marked cracks were taken before reopening the crack (previously healed crack), immediately after re-cracking, and after 2 and 5 weeks of incubation using a digital microscope (Celestron, Torrance, CA, USA). Image binarization was conducted using the commercially available image processing program ImageJ to determine the healing ratio [28]. After defining a black threshold level of 100, the healing ratio was measured as the decrease in the fraction area of each crack identified by black pixels immediately after cracking and at the final age (i.e., 5 weeks). Similar threshold values have been used in previous studies when using this binarization method to evaluate healing efficiency [21,29].

The healing ratio percentage was calculated according to Equation (1):

$$\text{Healing Ratio (\%)} = \frac{\left(A_i - A_f\right)}{A_i} \times 100 \tag{1}$$

where for an individual crack of a specific mortar prism, A_i = initial area and A_f = final area. The use of image binarization to quantify crack areas when investigating self-healing cementitious materials has been shown to accurately identify the crack and calculate its area with high precision [28,29].

A water-flow test, based on RILEM test Method 11.4 [30], was used to calculate the recovery of the water penetration resistance of the mortar prisms to quantify the ability of the cracks to regain the water tightness observed when these mortar prisms were previously healed. Tests were carried out before re-cracking (previously healed condition),

immediately after re-cracking, and at 5 weeks of healing. The water-flow coefficient, k, was calculated according to Equation (2) [16]:

$$k = \frac{aL}{A_t} \ln\left[\frac{h_1}{h_2}\right] \tag{2}$$

where k = water-flow coefficient (cm/s); a = cross-sectional area of the plastic cylinder (1.13 cm^2); L = depth of mortar prism (4 cm); A = cross-sectional contact area (9.62 cm^2); t = time (s); h_1 = initial water head (12.5 cm); and h_2 = final water head (cm).

2.3. New Crack Produced on 22-Month-Old Mortar Prisms

After conducting the re-healing study mentioned in Section 2.2, these same mortar prisms (nine specimens in total) were left to dry in room conditions for one week before generating a completely new crack on the top surface of the mortars. The aim of forming a new crack on these 22-month-old mortar specimens was to evaluate the ability of the initially encapsulated bacterial spores (in ACG particles) to successfully heal a new crack formed at a later age. A notch of approximately 2 mm depth was sawn perpendicular to the original crack to induce the crack formation within this notch (Figure 1). Then, a load was applied on the top of the mortar prisms to produce new cracks of approximately 0.5 mm width. The new cracks were produced following the processes explained above for reopening the previously healed cracks. The crack width was controlled for all samples by using plastic spacers with 0.5 mm thickness. A permanent blue marker pen was used to indicate two specific crack locations (per mortar prism) to enable monitoring of the crack at the same site. Once the new crack was formed and the locations marked, the specimens were prepared, incubated, and analysed following the same processes explained in the above section for re-cracking. Photos were taken of freshly cracked mortars (new cracks) and after 1, 4, and 8 weeks of healing, while the healing ratio was determined using the post-cracking and the 8-week crack areas. Water-flow tests were conducted immediately after cracking and after 4 and 8 weeks of healing. The healing percentage obtained from the water-flow tests was calculated according to Equation (3):

$$\text{Healing percentage (\%)} = \frac{(k_0 - k_t)}{k_0} \times 100 \tag{3}$$

where k_0 = initial water-flow after cracking, and k_t = water-flow at healing time t.

Furthermore, for each mortar specimen, three crack widths (in millimetres) were taken at the same location in the two points marked with the blue permanent marker (six measurements per sample) at different healing times (post-cracking, and 1, 4, and 8 weeks). The mean crack width for the complete crack was calculated by averaging these six measurements, while the healing (crack closure) percentage was calculated for each location according to Equation (4):

$$\text{Healing (crack width) \%} = \frac{(Cw_i - Cw_t)}{Cw_i} \times 100 \tag{4}$$

where Cw_i = initial crack width, and Cw_t = width measured at time t.

3. Results

In this study, two methods were used to evaluate the self-healing efficiency of the mortar prisms: quantification of the decrease in crack area and water-flow tests. The former has the benefits of being quick and non-destructive, while the latter is key to evaluating the recovery of water tightness [31].

3.1. Re-Cracking of Previously Healed 20-Month-Old Mortar Prisms

Three crack width measurements were taken at three different locations for each of the two points initially marked with a permanent pen on each mortar prism. In total,

18 measurements were taken for each of the three mortar mixes. Immediately after re-cracking the previously healed cracks, measurements of the crack widths were obtained in these locations. The mean crack widths observed for the Reference, Control, and Bio mortar mixes were 0.41 mm, 0.44 mm, and 0.38 mm, respectively.

3.1.1. Crack Area Quantification

After the initially healed cracks were reopened to a crack width of approximately 0.40 mm, soaked in a nutrients/calcium solution, and incubated semi-submerged in water for 5 weeks, no significant "new" healing was observed in any of the mortar prisms of the three different mixes (Figures 2 and 3).
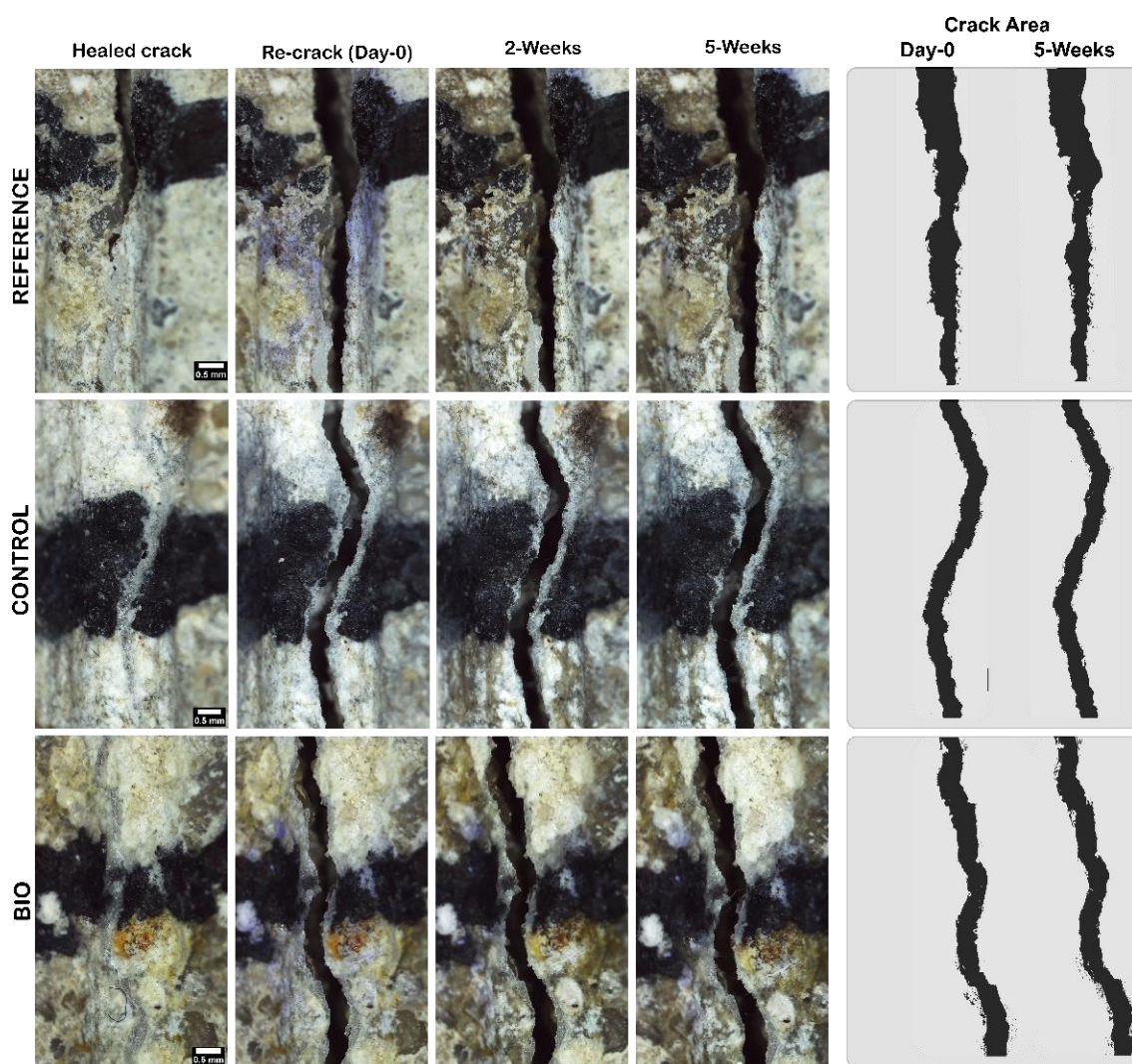

Figure 2. Re-crack closure in 20-month-old Reference, Control, and Bio mortars. Scale bar = 0.5 mm. Cracks in mortar specimens are shown after original healing (September 2019), immediately after re-cracking (February 2021), and after 2 and 5 weeks of incubation. Cracks were initially marked with a permanent black pen to allow the same region to be monitored over time. All images were taken with the same initial parameters to avoid post-manipulation.
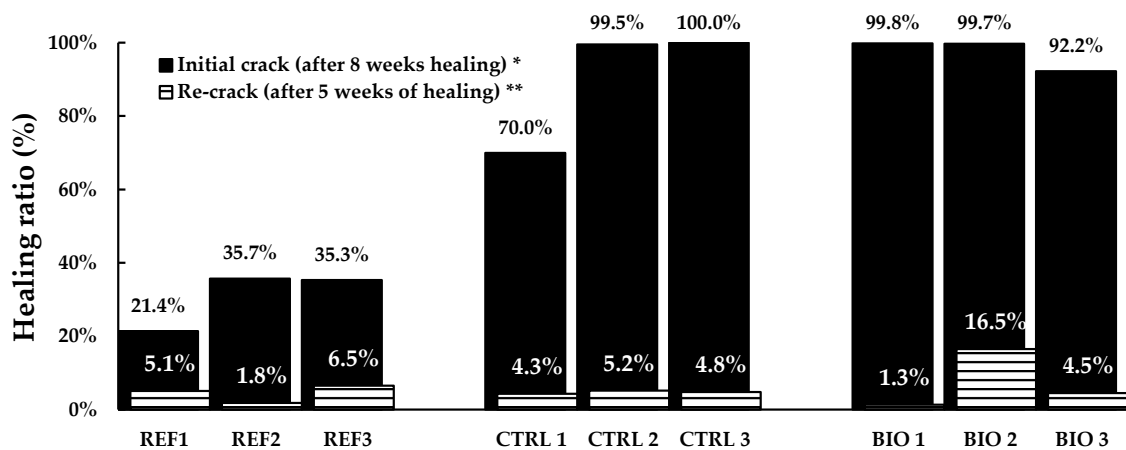
Figure 3. Healing ratio (%) of re-cracked mortar prisms (⊟), obtained as a function of crack area reduction, when compared with the healing ratio (%) obtained for initially healed cracks (■) as a function of the recovery of water tightness [9]. * Healing ratio as a function of reduction in water tightness. ** Healing ratio as a function of reduction in the area of the crack.

3.1.2. Water Tightness

Water-flow tests were carried out on the previously healed crack immediately after the re-cracking process and after 5 weeks of incubation. Intermediate water-flow tests were not performed to avoid accidentally removing any newly formed precipitates, as suggested by other authors [31]. Figure 4 shows the average water-flow coefficient (k) for the original crack and healed crack [9] along with the values obtained in this study immediately after re-cracking and after 5 weeks of healing of the reopened crack.
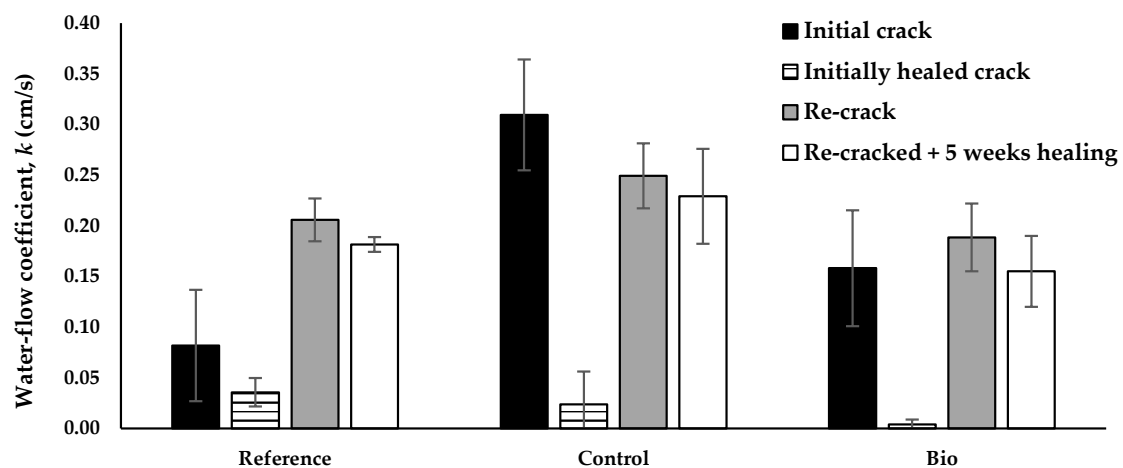

Figure 4. Comparison of the water-flow coefficients (k) of the three different mortar mixes (Reference, Control, and Bio): initially cracked (■) and after initial healing for 8 weeks (⊟) as reported by [9]; and from this study, immediately after re-cracking (■) and after re-cracked and healed for 5 weeks (□).

It was observed that none of the mortar prisms were able to recover the water-flow coefficient observed on the previously healed cracks after they were re-cracked. Moreover, no significant reduction was observed in the water-flow coefficient between the time when the crack was immediately re-cracked and 5 weeks later, and these results were consistent with the crack area quantification results (Figure 3).

3.2. *New Cracks Produced on 22-Month-Old Mortar Prisms*

In a similar way to the re-cracking of previously healed cracks, three crack width measurements of the newly formed cracks were taken at three different locations for each

of the two points marked with a permanent pen. The crack width of these newly formed cracks was measured immediately after cracking, and the mean crack widths observed for the Reference, Control, and Bio mortar mixes were 0.44 mm, 0.43 mm, and 0.45 mm, respectively. In addition to measuring the crack width immediately after cracking, the crack widths at these exact locations (18 locations per mortar mix) were also measured after 1, 4, and 8 weeks of healing. In total, 54 measurements were performed at each healing age covering the three different mortar mixes (Reference, Control, and Bio). The crack healing percentage was then calculated for each location according to Equation (4). The initial crack width of each crack location in relation to its healing percentage (crack closure) obtained after 8 weeks of healing is presented in Figure 5.
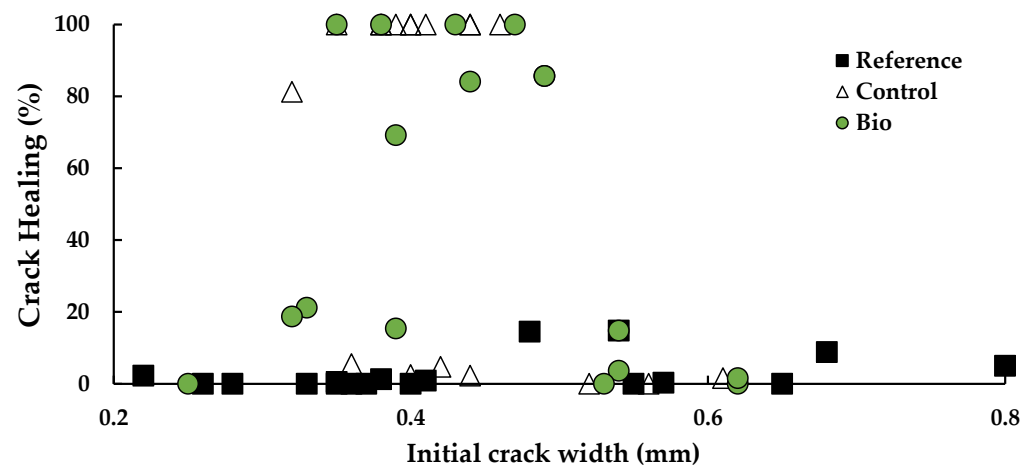

Figure 5. Crack healing (%) as a function of the initial crack width for newly formed cracks on 22-month-old mortar prisms. Results are plotted from 9 cracks (54 measurements) of the three mortar mixes (Reference, Control, and Bio) after a healing time of 8 weeks.

3.2.1. Crack Area Quantification

After being incubated for 7 days, healing of newly formed cracks was observed in the Bio mortar prisms, and some crystal formations were also observed in the Control mix. Moreover, after 4 weeks, Bio mortar prisms presented almost a complete closure of the new cracks, while the Control specimens did not present any significant improvement when compared with the healing observed after one week of incubation. In contrast, no crystals were formed inside the new cracks nor was healing observed in any of the three Reference samples at any time during the incubation process. Binary images of the post-cracking and 8-week-old new cracks were analysed using ImageJ software. In Figure 6, a representative crack is presented for each mortar mix.
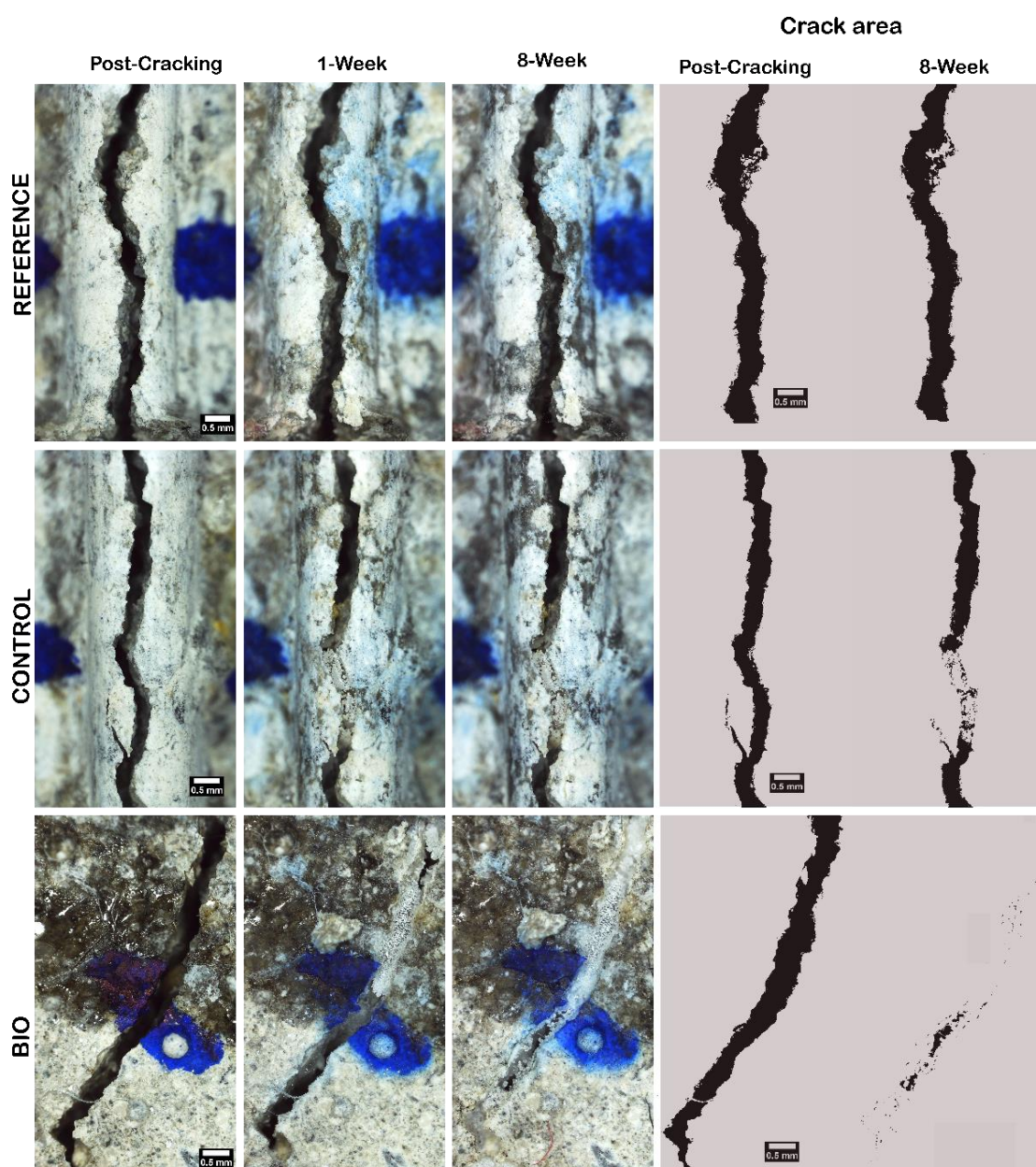
Figure 6. New crack healing in representative Reference, Control, and Bio mortar prisms. Scale bar = 0.5 mm. On the left, new cracks are shown immediately after cracking, followed by 1-week and 8-week incubation. On the right, binary images of the post-cracking and 8-week-old new cracks were analysed using ImageJ software. All images were taken with the same initial parameters to avoid post-manipulation.

The mean healing ratios for the new cracks produced on the 22-month-old mortar prisms are presented in Figure 7. Contrary to what was observed when re-cracking the previously healed cracks, some healing was observed on the 22-month-old Control mortar prisms when new cracks were produced. As the mortar prisms were not kept in sterile conditions to more closely replicate commercial applications, the healing ratio observed for the Control samples likely originated from the presence of environmental bacteria. These bacteria may have been able to utilize either the nutrients and calcium precursors embedded within the freshly open mortar matrix (i.e., added when mortars were initially cast) or the additional nutrients added when these new cracks were submerged in the GM solution [9].
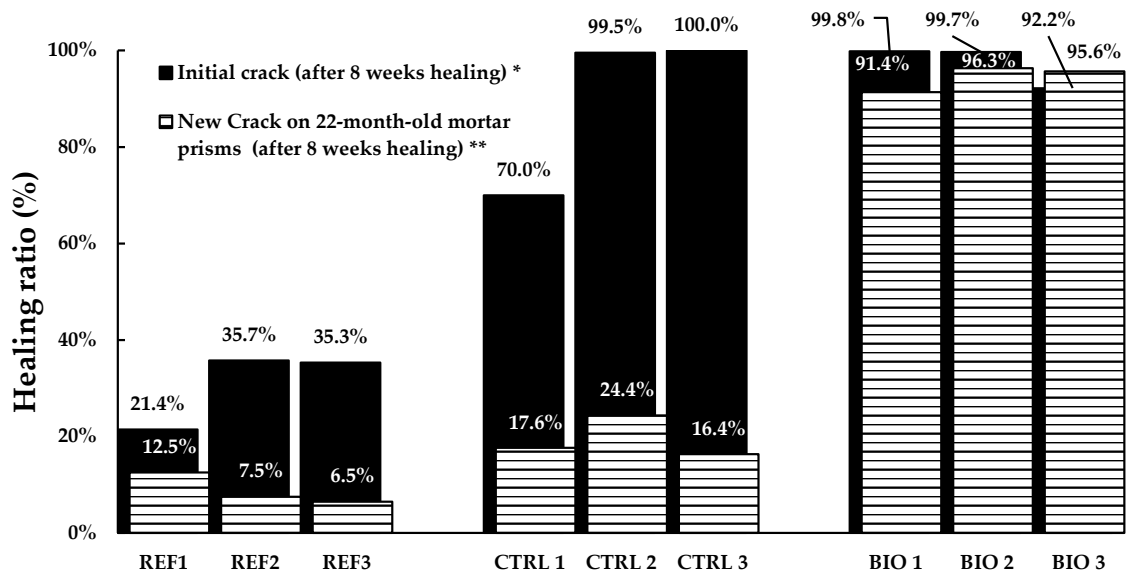
Figure 7. Healing ratio (%) of 22-month-old newly cracked mortar prisms ($=$), obtained as a function of crack area reduction, when compared with the healing ratio (%) obtained for initially healed cracks (■) as a function of the recovery of water tightness reported by [9]. * Healing ratio as a function of reduction in water tightness. ** Healing ratio as a function of reduction in the area of the crack.

3.2.2. Water Tightness

Water-flow tests were carried out on the newly formed cracks immediately after the cracking process and after 5 and 8 weeks of incubation. Water-flow tests at early ages (i.e., 7, 14, and 21 days) were not performed to avoid removing any newly formed precipitates [31]. The percentages of crack healing as a function of the reduction in the water-flow coefficient after 5 and 8 weeks of healing for each of the three mortar mixes are shown in Figure 8. These healing percentage results were consistent with the decrease in the crack area obtained via image binarization.
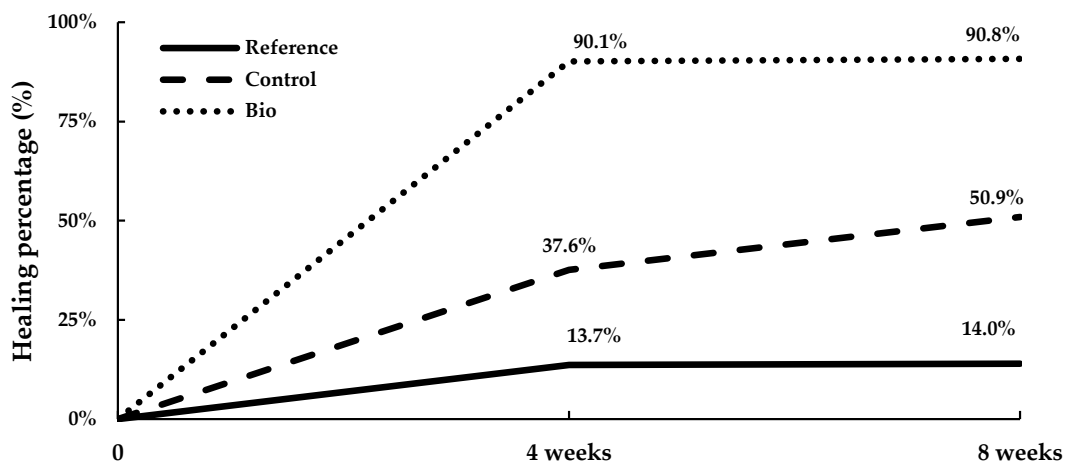

Figure 8. Healing percentage (%) of mortar prisms in terms of reduction in water-flow coefficient (*k*) for new cracks of the following three mortar mixes: Reference, Control, and Bio. Mortar prisms were evaluated immediately after the new crack was formed and after 4 and 8 weeks of healing. Results represent the average of three mortar prisms for each mortar mix at 4 and 8 weeks of healing.

4. Discussion

4.1. Re-Cracking of Previously Healed 20-Month-Old Mortar Prisms

The results show that the cement mortar cracks that were successfully healed at an early age were not able to successfully re-heal when they were re-cracked 20 months later and exposed to extremely favourable conditions (i.e., high humidity, temperature, calcium source, and nutrients) to promote their re-healing. The abovementioned results may be directly related to the number of viable spores available within the reopened crack. It is well known that a minimum spore concentration is required to ensure high efficiency of calcium precipitation in BBSH cementitious composites [5,32,33]. Therefore, it is likely that the number of viable spores on the freshly reopened crack was insufficient to start a new healing cycle. In this regard, different causes could have led to not having the required minimum spore concentration. On the one hand, it is possible that the original vegetative bacteria cells, responsible for the first healing cycle, were not able to successfully sporulate again during the initial healing. On the other hand, even if the bacteria did successfully sporulate within the crack, the spores could be permanently trapped within the $CaCO_3$ precipitates or exposed to environmental conditions (e.g., flowing water) that could potentially remove them from the crack surface. Regarding the latter possibility, further research is needed to elucidate whether water flowing through the cracks, as occurs in water-flow tests usually conducted to evaluate the water tightness during the healing process, is likely responsible for removing part of the spores needed for a new healing cycle to occur in these healed cracks.

In summary, it is probable that after 20 months, insufficient bacterial spores were available within the initially healed crack to successfully start a new self-healing cycle. The biggest challenge to achieve cyclic healing is not only to guarantee that enough spores are produced and successfully protected during the first healing cycle but also to ensure that nutrients and calcium precursors for the new generation of bacteria are readily available once the healed crack is reopened. In this regard, it appears that bacteria-based cyclic healing would only be possible if either new ways could be found to re-introduce fresh bacteria along with nutrients and calcium, or the protection method could be designed such that not all bacterial spores, nutrients, and additional calcium are released upon a single cracking event. For the latter, a very promising protection method could be the use of dual-channel mini-vascular networks (MVNs) [34]. De Nardi et al. [35] have demonstrated the feasibility of these MVNs when using chemical healing agents (i.e., sodium silicate). These MVNs, consisting of interconnected hollow ligaments, can act as healing agent reservoirs that are able to release the healing agents during multiple damage-healing events. Therefore, dual-channel MVNs could potentially be able to independently store spores and nutrients, and release them after multiple occurrences of damage.

4.2. New Cracks Produced on 22-Month-Old Mortar Prisms

Over the past decade, a wide variety of carriers have been investigated in depth for their ability to protect bacterial spores [5,25,36]. However, most of this research has been conducted to guarantee that these carriers can protect the spores from the initial harsh conditions and deliver them once an early crack is formed, generally after 28 days. Therefore, less attention has been given to the long-term protection efficiency of these carriers for cracks formed at a later age (i.e., more than 28 days). Among the few studies on long-term protection efficiency, Zheng and Qian [37] investigated two kinds of low alkaline materials (potassium magnesium phosphate (MKPC) and sulphoaluminate cement (SC)) as protective carriers of bacterial spores for cracks formed in 6-month-old mortar samples. They observed that these protective carriers were able to safeguard the spores and successfully achieve self-healing of later-age cracks. Other studies have demonstrated the feasibility of using ACGs to protect bacterial spores when cracks are formed in 9-month-old mortar prisms [21,38].

In this context, the present study investigated for the first time the long-term efficiency of this specific protective carrier (i.e., ACGs) when a new crack is formed in 22-month-old

mortar prisms. It was demonstrated that the bacterial spores encapsulated within the ACGs remained viable inside the cementitious matrix and were successfully activated when the proper conditions were supplied (i.e., nutrients, additional calcium, water, and oxygen). As a result, the new cracks (0.45 mm width) achieved an average healing ratio and water tightness recovery of 93.3% and 90.8%, respectively (Figures 7 and 8). In this regard, the cracks were not able to achieve a healing ratio of 100%, likely as a result of not enough bacteria-laden ACG particles being hit when the new crack was formed. This resulted in likely not enough spores being released to achieve a complete crack closure. Nevertheless, the overall results imply that when bacterial spores and the required nutrients are independently protected using proven protection methods (i.e., ACGs), BBSH could be a viable long-term alternative for healing one-event cracks occurring at a significantly later age. Nevertheless, further research is needed to elucidate the shelf-life of both the spores and the nutrients protected inside the cement matrix so that the simultaneous release of both components in the presence of water and oxygen can allow the successful healing of a later-age crack.

5. Conclusions

The purpose of this study was, on the one hand, to investigate the capability of BBSH cementitious materials to successfully re-heal previously healed cracks when these cracks are reformed at a later age (i.e., 20 months); and, on the other hand, to evaluate the viability of encapsulated bacterial spores when new cracks are generated on 22-month-old mortar samples. The following key conclusions can be drawn:

1. It has been demonstrated that bacterial spores encapsulated into ACGs remain viable within the cement matrix and can heal later-formed cracks (at 22 months) if proper conditions are supplied (i.e., nutrients, additional calcium, and humidity).
2. The BBSH mortar formulation investigated, where spores from a bacterium closely related to *Bacillus licheniformis* were encapsulated into aerated concrete granules (ACGs), is not effective for re-healing previously healed cracks when these are reformed at a later age (i.e., 20 months).
3. The lack of healing observed when the cracks were reformed is likely due to the absence of enough viable bacterial spores available within the reopened cracks. In this regard, further research is needed to elucidate whether the bacteria, capable of healing the cracks in the first instance, can form new spores and whether these new spores can remain protected within the calcium carbonate precipitates formed during the first healing cycle.
4. Therefore, for one-time healing events, independent encapsulation of spores and nutrients might allow efficient healing. However, for successful cyclic healing, additional research should be conducted on developing systems capable of effective repetitive delivery of spores and nutrients (e.g., vascular networks).

Author Contributions: Conceptualization, I.J.-R., S.G. and K.P.; methodology, I.J.-R., S.G. and K.P.; formal analysis, I.J.-R.; investigation, I.J.-R. and B.J.R.; resources, A.H., S.G. and K.P.; data curation, I.J.-R. and B.J.R.; writing—original draft preparation, I.J.-R.; writing—review and editing, B.J.R., A.H., S.G. and K.P.; visualization, I.J.-R. and B.J.R.; supervision, A.H., S.G. and K.P.; project administration, K.P.; funding acquisition, S.G. and K.P. All authors have read and agreed to the published version of the manuscript.

Data Availability Statement: All data relevant to this study are reported in the Results section of this publication.

Conflicts of Interest: The authors declare no conflict of interest. The funders had no role in the design of the study; in the collection, analyses, or interpretation of data; in the writing of the manuscript, or in the decision to publish the results.

References

1. Mehta, P.; Monteiro, P.J. *Concrete: Microstructure, Properties, and Materials*, 3rd ed.; Mc Graw Hill: New York, NY, USA, 2006; p. 659.
2. Zongjin, L. *Advanced Concrete Technology*; John Wiley & Sons, Inc.: Hoboken, NJ, USA, 2011.
3. Seifan, M.; Samani, A.K.; Berenjian, A. Bioconcrete: Next generation of self-healing concrete. *Appl. Microbiol. Biotechnol.* **2016**, *100*, 2591–2602. [CrossRef] [PubMed]
4. De Belie, N.; Gruyaert, E.; Al-Tabbaa, A.; Antonaci, P.; Baera, C.; Bajare, D.; Darquennes, A.; Davies, R.; Ferrara, L.; Jefferson, T. A review of self-healing concrete for damage management of structures. *Adv. Mater. Interfaces* **2018**, *5*, 1800074. [CrossRef]
5. Justo-Reinoso, I.; Heath, A.; Gebhard, S.; Paine, K. Aerobic non-ureolytic bacteria-based self-healing cementitious composites: A comprehensive review. *J. Build. Eng.* **2021**, *42*, 102834. [CrossRef]
6. Farhadi, S.; Ziadloo, S. Self-Healing Microbial Concrete—A Review. In *Materials Science Forum*; Trans Tech Publications Ltd.: Bäch, Switzerland, 2020; Volume 990, pp. 8–12.
7. Kim, H.; Son, H.; Seo, J.; Lee, H.-K. Recent advances in microbial viability and self-healing performance in bacterial-based cementitious materials: A review. *Constr. Build. Mater.* **2021**, *274*, 122094. [CrossRef]
8. Tziviloglou, E.; Wiktor, V.; Jonkers, H.M.; Schlangen, E. Selection of nutrient used in biogenic healing agent for cementitious materials. *Front. Mater.* **2017**, *4*, 15. [CrossRef]
9. Reeksting, B.J.; Hoffmann, T.D.; Tan, L.; Paine, K.; Gebhard, S. In-depth profiling of calcite precipitation by environmental bacteria reveals fundamental mechanistic differences with relevance to application. *Appl. Environ. Microbiol.* **2020**, *86*, e02739-19. [CrossRef]
10. Yoonhee, J.; Wonjae, K.; Wook, K.; Woojun, P. Complete Genome and Calcium Carbonate Precipitation of *Alkaliphilic bacillus* sp. AK13 for Self-Healing Concrete. *J. Microbiol. Biotechnol.* **2020**, *30*, 404–416. Available online: http://kiss.kstudy.com/search/detail_page.asp?key=3761121 (accessed on 22 April 2022).
11. Zhu, T.; Dittrich, M. Carbonate precipitation through microbial activities in natural environment, and their potential in biotechnology: A review. *Front. Bioeng. Biotechnol.* **2016**, *4*, 4. [CrossRef]
12. Shashank, B.; Dhannur, B.; Ravishankar, H.; Nagaraj, P. Study on Development of Strength Properties of Bio-concrete. In *Sustainable Construction and Building Materials*; Springer Nature Singapore Pte Ltd.: Singapore, 2019; pp. 423–437.
13. Roig-Flores, M.; Formagini, S.; Serna, P. Self-healing concrete—What Is it Good For? *Mater. Constr.* **2021**, *71*, e237. [CrossRef]
14. Wang, J.; Soens, H.; Verstraete, W.; De Belie, N. Self-healing concrete by use of microencapsulated bacterial spores. *Cem. Concr. Res.* **2014**, *56*, 139–152. [CrossRef]
15. Pacheco-Torgal, F.; Melchers, R.; de Belie, N.; Shi, X.; Van Tittelboom, K.; Perez, A.S. *Eco-Efficient Repair and Rehabilitation of Concrete Infrastructures*; Woodhead Publishing: Sawston, UK, 2017.
16. Tan, L.; Reeksting, B.; Ferrandiz-Mas, V.; Heath, A.; Gebhard, S.; Paine, K. Effect of carbonation on bacteria-based self-healing of cementitious composites. *Constr. Build. Mater.* **2020**, *257*, 119501. [CrossRef]
17. Rauf, M.; Khaliq, W.; Khushnood, R.A.; Ahmed, I. Comparative performance of different bacteria immobilized in natural fibers for self-healing in concrete. *Constr. Build. Mater.* **2020**, *258*, 119578. [CrossRef]
18. Han, S.; Jang, I.; Choi, E.K.; Park, W.; Yi, C.; Chung, N. Bacterial Self-Healing Performance of Coated Expanded Clay in Concrete. *J. Environ. Eng.* **2020**, *146*, 04020072. [CrossRef]
19. Zhu, X.; Mignon, A.; Nielsen, S.D.; Zieger, S.E.; Koren, K.; Boon, N.; De Belie, N. Viability determination of *Bacillus sphaericus* after encapsulation in hydrogel for self-healing concrete via microcalorimetry and in situ oxygen concentration measurements. *Cem. Concr. Compos.* **2021**, *119*, 104006. [CrossRef]
20. Gao, M.; Guo, J.; Cao, H.; Wang, H.; Xiong, X.; Krastev, R.; Nie, K.; Xu, H.; Liu, L. Immobilized bacteria with pH-response hydrogel for self-healing of concrete. *J. Environ. Manag.* **2020**, *261*, 110225. [CrossRef]
21. Justo-Reinoso, I.; Reeksting, B.J.; Hamley-Bennett, C.; Heath, A.; Gebhard, S.; Paine, K. Air-entraining admixtures as a protection method for bacterial spores in self-healing cementitious composites: Healing evaluation of early and later-age cracks. *Constr. Build. Mater.* **2022**, *327*, 126877. [CrossRef]
22. Erşan, Y.Ç.; Da Silva, F.B.; Boon, N.; Verstraete, W.; De Belie, N. Screening of bacteria and concrete compatible protection materials. *Constr. Build. Mater.* **2015**, *88*, 196–203. [CrossRef]
23. Luo, J.; Chen, X.; Crump, J.; Zhou, H.; Davies, D.G.; Zhou, G.; Zhang, N.; Jin, C. Interactions of fungi with concrete: Significant importance for bio-based self-healing concrete. *Constr. Build. Mater.* **2018**, *164*, 275–285. [CrossRef]
24. Mors, R.; Jonkers, H. Effect on concrete surface water absorption upon addition of lactate derived agent. *Coatings* **2017**, *7*, 51. [CrossRef]
25. Lee, Y.S.; Park, W. Current challenges and future directions for bacterial self-healing concrete. *Appl. Microbiol. Biotechnol.* **2018**, *102*, 3059–3070. [CrossRef]
26. Kua, H.W.; Gupta, S.; Aday, A.N.; Srubar, W.V., III. Biochar-immobilized bacteria and superabsorbent polymers enable self-healing of fiber-reinforced concrete after multiple damage cycles. *Cem. Concr. Compos.* **2019**, *100*, 35–52. [CrossRef]

27. Šavija, B.; Luković, M. Carbonation of cement paste: Understanding, challenges, and opportunities. *Constr. Build. Mater.* **2016**, *117*, 285–301. [CrossRef]

28. Stefanidou, M.; Tsampali, E.; Karagiannis, G.; Amanatiadis, S.; Ioakim, A.; Kassavetis, S. Techniques for recording self-healing efficiency and characterizing the healing products in cementitious materials. *Mater. Des. Process. Commun.* **2021**, *3*, e166. [CrossRef]

29. Luo, M.; Qian, C.-X.; Li, R.-Y. Factors affecting crack repairing capacity of bacteria-based self-healing concrete. *Constr. Build. Mater.* **2015**, *87*, 1–7. [CrossRef]

30. RILEM. *RILEM Test Method 11.4: Measurement of Water Absorption under Low Pressure*; RILEM: Paris, France, 1987.

31. Roig-Flores, M.; Pirritano, F.; Serna, P.; Ferrara, L. Effect of crystalline admixtures on the self-healing capability of early-age concrete studied by means of permeability and crack closing tests. *Constr. Build. Mater.* **2016**, *114*, 447–457. [CrossRef]

32. Zhang, J.; Mai, B.; Cai, T.; Luo, J.; Wu, W.; Liu, B.; Han, N.; Xing, F.; Deng, X. Optimization of a binary concrete crack self-healing system containing bacteria and oxygen. *Materials* **2017**, *10*, 116. [CrossRef]

33. Alazhari, M.; Sharma, T.; Heath, A.; Cooper, R.; Paine, K. Application of expanded perlite encapsulated bacteria and growth media for self-healing concrete. *Constr. Build. Mater.* **2018**, *160*, 610–619. [CrossRef]

34. De Nardi, C.; Gardner, D.; Jefferson, T. *Advanced 3D Printed Mini-Vascular Network for Self-Healing Concrete*; Maddalena, R., Wright-Syed, M., Eds.; Cardiff University: Cardiff, UK, 2021; p. 292.

35. De Nardi, C.; Gardner, D.; Jefferson, A.D. Development of 3D printed networks in self-healing concrete. *Materials* **2020**, *13*, 1328. [CrossRef]

36. Indhumathi, S.; Dinesh, A.; Pichumani, M. Diverse perspectives on self healing ability of Engineered Cement Composite—All-inclusive insight. *Constr. Build. Mater.* **2022**, *323*, 126473.

37. Zheng, T.; Qian, C. Self-healing of later-age cracks in cement-based materials by encapsulation-based bacteria. *J. Mater. Civ. Eng.* **2020**, *32*, 04020341. [CrossRef]

38. Skevi, L.; Reeksting, B.; Gebhard, S.; Paine, K. Bacteria Based Self-healing of Later-Age Cracks in Concrete. In *International RILEM Conference on Early-Age and Long-Term Cracking in RC Structures*; Springer International Publishing: Cham, Switzerland, 2021; pp. 367–376.